

MODELLING OF THE HYDRATION AND MOISTURE TRANSFER COUPLING EFFECTS ON THE MICROSTRUCTURE PROPERTIES OF THE CONCRETE COVER

Z. Zhang, M. Thiery, V. Baroghel-Bouny, M.D. Nguyen, P. Rossi

Paris-Est University; IFSTTAR (former LCPC), Materials Department, Paris

Abstract

In this research, a model of the couplings between hydration and moisture transfer within cementitious materials is proposed. Based on taking into account the microstructure properties and the moisture transfer properties due to hydration, the model describes the couplings between the moisture transfer at early-age owing to external drying and the internal water depletion by hydration. Furthermore, the slowing down of the hydration kinetics caused by the decrease of relative humidity prevailing in the pores is also investigated. Experimental data, such as drying kinetics, as well as porosity and degree of hydration profiles, are used to verify the proposed modelling. The materials used here are three OPC cement pastes with different water-to-cement ratios. The agreement between observed and modelled results is considered satisfactory and confirms the possibilities of using the coupling model to simulate moisture transfer for cementitious materials at early-age.

Key words: hydration, moisture transfers, early-age, microstructure, moisture properties, modelling

1. INTRODUCTION

After the formwork removal, the concrete structure is exposed to the surrounding where the relative humidity (RH) is less than that within the material. On the one hand, this disequilibrium results in a movement of moisture from the internal to the external, leading to drying of the material. On the other hand, since hydration needs water, early drying can affect the microstructure of the material and slow the hydration kinetics down.

Aiming at developing a coupling model, the basic idea is to couple the kinetics of water consumption by hydration with the moisture transfers. The DuCom model, developed by Maekawa et al. [1], describes the hydration process as the evolution of hydration degree for each clinker phase. The development of the microstructure during hydration is reflected by hydration degree. However, with regard to microstructure, only the evolution of porosity is taken into account in this model. Bentz et al. [2] have proposed a model to simulate interactions between water evaporation in the pores due to the drying process and hydration kinetics. The empiricism (non-systematic approach) and the lack of flexibility cause that modelling results do not agree with observed data very well. Buffo-Lacarriere et al. [3] consider that the kinetics of hydration for each anhydrous phase is influenced by the availability of water and neglect the influence of the evolution of microstructure on moisture properties because it is admitted that the moisture transfer at the early-age remains low.

This paper presents a coupling model which is derived from an isothermal drying model where transport coefficients are dependent on the degree of hydration (α). The hydration kinetics is taken into account by considering the diffusion-control step of hydration. Some of the experimental data in this paper are taken from Nguyen's thesis [4]. The materials, used to verify the model, are OPC pastes, CO, CN and CP, and water-to-cement ratios are 0.35, 0.45 and 0.60, respectively [5]. The drying experiments start as in the case of formwork removal (after one-day curing), and the specimens are submitted to a laboratory environment (external RH = 50 ± 5% and temperature $T = 293 \pm 1$ K).

2. ISOTHERMAL DRYING MODEL

2.1 Balance equations and transport equations

An isothermal drying model can be developed based on two assumptions. First, the total gas pressure in the medium is constant and equal to the atmospheric pressure during the drying ($p_g = p_{atm}$). Second, the moisture transfer described by a single diffusion equation with a global moisture transfer coefficient ($D(S_l) = D_l(S_l) + D_v(S_l)$), including the movement of liquid water ($D_l(S_l)$) and the diffusion of water vapor ($D_v(S_l)$) [6, 7].

$$\phi \frac{\partial S_l}{\partial t} = -\text{div}(D(S_l)\text{grad } S_l) \quad (1)$$

where

$$D_l(S_l) = \frac{dp_c(S_l)}{dS_l} \frac{K_l k_{rl}(S_l)}{\eta_l} \quad (2)$$

$$D_v(S_l) = \frac{dp_c(S_l)}{dS_l} \frac{f(\phi, S_l) D_{va}}{p_v} \left(\frac{\rho_v}{\rho_l} \right)^2 \quad (3)$$

where S_l is the degree of liquid water saturation, the coefficient K_l represents the intrinsic liquid water permeability, η_l is the dynamic viscosity of liquid water, ρ_v and ρ_l stand for the density of water vapor and liquid water respectively, p_v and $p_c(S_l)$ represent the water vapor pressure and the capillary pressure, k_{rl} is the relative permeability (dimensionless) of liquid water and varies between 0 and 1, $f(\phi, S_l)$ is the gas diffusion resistance factor, which depends on the porosity (ϕ) and S_l . In Eq. (3), D_{va} is the free water vapor diffusion coefficient in the air and it is $2.47 \times 10^5 \text{ m}^2 \cdot \text{s}^{-1}$ ($T = 293 \pm 1$ K and $p_g = p_{atm}$) in this paper [7].

Among the various expressions of $f(\phi, S_l)$, the one proposed by Millington [8] for granular materials has been widely used for partially saturated porous media [4, 7].

$$f(\phi, S_l) = \phi^a (1 - S_l)^b \quad (4)$$

where a and b are two parameters related to gaseous constituents and the tortuosity effects. Thiéry et al. [9] suggest $a = 2.74$ and $b = 4.20$, providing a much better fitting on the basis of the Papadakis [10] and Sercombe [11] experimental measurements. In this paper, the values proposed by Thiéry et al. are used.

2.2 Constitutive equations

(1) Capillary Pressure

Generally, the capillary pressure is considered as a function of RH and can be expressed by the Kelvin law.

$$p_c = -\frac{\rho_l RT}{M_v} \ln \text{RH} \quad (5)$$

where M_v and R are the molar mass of water vapor and the ideal gas constant, respectively. At the macroscopic scale, p_c is the difference between the gas pressure (p_g) and liquid water pressure (p_l): $p_c = p_g - p_l$.

(2) Relative permeability

The Mualem model [12] is applied to derive the relative permeability of liquid water ($k_{rl}(S_l) = S_l^{1/2}[KL + (1 - KL)KH]^2$), which is given by two normalized integral functions using the capillary pressure as input data: $KL(S_l) = (\int_{p_c}^{+\infty} dL/(S_l)p_c^2)/(\int_0^{+\infty} dL/(S_l)p_c^2)$ and $KH(S_l) = (\int_{p_c}^{+\infty} dH/(S_l)p_c^2)/(\int_0^{+\infty} dH/(S_l)p_c^2)$.

The literature (see [4] and [13]) describes this model in more details.

3. COUPLING MODEL BETWEEN DRYING AND HYDRATION

The hydration model used here is based on Bernard's work [14], which is able to take into account the hydration kinetics of each clinker phase in the presence of gypsum and the effects of water content on the evolution of hydration. The Fuji and Kondo's model [15] is employed to address the effect of the reduction in accessibility due to the hydrates formation on the hydration kinetics of each clinker phase. The model is detailed in the literature [4].

A coupling occurs through the evolution of the microstructure during the hydration of the material, which directly influences the moisture transfer. Actually, the development of the microstructure has a strong influence on the moisture transfers through the evolution of porosity ($\phi(\alpha)$), the intrinsic ($K_l(\alpha)$) and relative permeability ($k_{rl}(S_l, \alpha)$), and the capillary pressure curve ($p_c(S_l, \alpha)$), etc.

3.1 Evolution of the porosity

The evolution of porosity at early-age has been described as a function of the degree of hydration by Delmi et al. for OPC materials as follows [16].

$$\phi(\alpha) = \phi_0 \left(1 - \frac{\alpha C_m}{4 W_m} \right) \quad (6)$$

where ϕ_0 is the porosity of the specimens just after the mixing, C_m and W_m are the mass of cement and of water referring to the mix-design.

3.2 Evolution of the intrinsic liquid water permeability

A relationship between the intrinsic permeability and the degree of hydration can be proposed by using the Katz-Thompson theory [17], which has been improved by Thiéry et al. [18] for cementitious materials,

$$-\log \left(\frac{K_l}{K_l^0} \right) = v(\alpha - \alpha_0) \quad (7)$$

where K_l^0 and K_l are the intrinsic liquid water permeability corresponding to the degree of hydration α_0 (after one-day curing) and α , respectively. v is the linear regression coefficient gained by fitting Eq. (7) with the measured data and it is given as 8.02 for CO, CN and CP.

3.3 Evolution of the desorption curve during hydration

The desorption curve describes the relationship between S_l (or water content w) and RH, which is modelled in this section. Furthermore, the expression of $p_c(S_l, \alpha)$ is rewritten based on the modelling of desorption curve, which also affects the prediction of $k_{rl}(S_l, \alpha)$ according to the analysis proposed in Section 2.2.

We define the normalized water content w^* as the mass of free water (m_l) divided by the mass of C-S-H (m_{CSH}).

$$w^* = \frac{m_l}{m_{CSH}} = w \frac{1 + \alpha\lambda}{\alpha\gamma^*} \quad (8)$$

where λ is the mass of water consumed by per gram of hydrated cement, γ^* is the mass of formed C-S-H by per gram of hydrated cement. The literature [4] has analysed the case of OPC materials with experimental water vapor desorption data from [7] and gave $\lambda = 0.42$ and $\gamma^* = 0.75$. Here, let's define $\psi(\alpha) = (1 + \alpha\lambda)/\alpha\gamma^*$.

The normalized desorption curve is considered as the relationship between w^* and RH (plotted in Fig. 1, see symbols). It is clearly seen that there are two distinguished regions on the curve. According to Baroghel-Bouny's research [7], a multi-layer adsorption of water molecules on the surface of the C-S-H plays a dominant role for low RH values and the capillary pore system is the most important parameter for the high RH values. These two regions are separated by a threshold RH value, which is around $RH_{lim} = 44\%$ in desorption [7].

For low RH values ($<RH_{lim}$), the curve is modelled by the van Genuchten equation [19].

$$w^* = (1 + (-c \ln RH)^n)^{-m} \quad (9)$$

A fitting procedure makes it possible to determine the following universal parameters: $c = 23.49$, $m = 0.45$ and $n = 1.82$ for OPC cement pastes. In the following, this region of normalized desorption curve will be denoted by VG (RH).

For high RH values ($>RH_{lim}$), the expression of w^* should be easy to describe the change of the normalized desorption curve and be simple enough to be inversed and derivative. An analytical equation according to α is chosen, which is a second-degree polynomial including three parameters.

$$w^* = A RH^2 + B RH + C \quad (10)$$

where parameters A, B and C, which depend on α and ϕ , are determined by the following three conditions.

(a). The curve must be continuous at RH_{lim} :

$$w^*(RH_{lim}) = A RH_{lim}^2 + B RH_{lim} + C = VG(RH_{lim}) \quad (11)$$

(b). The first derivative of the curve at RH_{lim} must also be continuous:

$$w^{*'}(RH_{lim}) = 2A RH_{lim} + B = VG'(RH_{lim}) \quad (12)$$

(c). When $RH = 100\%$, the water content is directly related to the bulk accessible-to-water porosity (ϕ) and is computed by using ρ_l and the bulk density of the saturated material (ρ_{app}).

$$w(RH=100\%) = w_{max} = \phi \frac{\rho_l}{\rho_{app}} \quad \text{with } \rho_{app} = (1 + \alpha\lambda) / \left(\frac{1}{\rho_c} + \frac{W_m}{C_m} \frac{1}{\rho_l} \right) \quad (13)$$

where ρ_c is the cement density. Hence, w^* for $RH = 100\%$ is imposed by the following equation:

$$w^*(RH=100\%) = A + B + C = \psi(\alpha) \frac{\rho_l}{\rho_{app}} \phi \quad (14)$$

Fig. 1 represents the numerical results of the normalized desorption curves, which are consistent with experimental data [7] obtained on the studied materials.

The dependence of w on the degree of hydration α is calculated by using Eq. (8). Desorption curves for CO and CN are shown in Fig. 2.

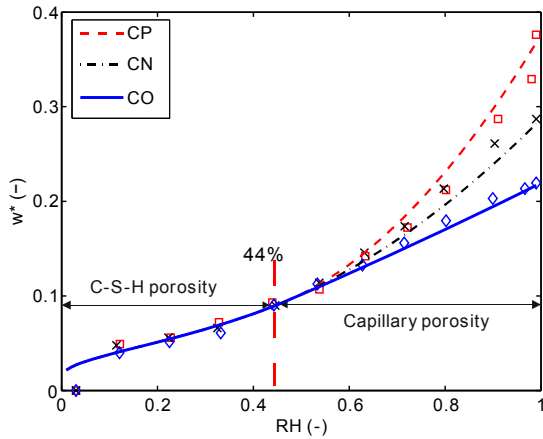


Fig. 1: Normalized desorption curves. Simulations (lines) and experiments [7] (symbols).

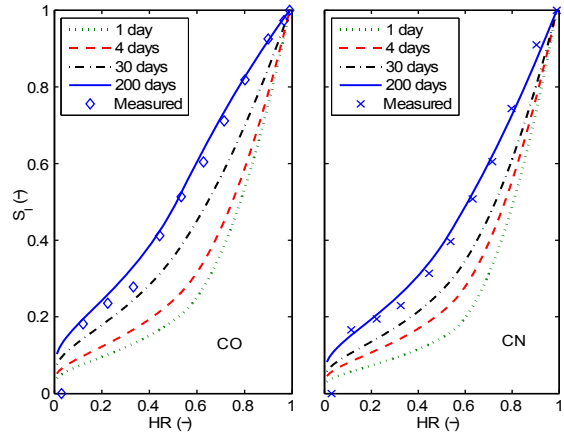


Fig. 2: Desorption curves for CO and CN at different ages. Comparison with measurements [7] obtained for fully hydrated cement pastes.

3.4 Evolution of the capillary pressure as function of the degree of hydration

Since the desorption curve is divided into two regions by a threshold RH value, the capillary pressure curve can be rewritten in two equations, according to the Kelvin law (see Ep. 5).

For $RH < RH_{lim}$:

$$p_c(S_l, \alpha) = \frac{\rho_l RT}{M_v} \frac{1}{\alpha} \left((\psi(\alpha) S_l w_{max})^{-1/m} - 1 \right)^{1/n} \quad (15)$$

For $RH \geq RH_{lim}$:

$$p_c(S_l, \alpha) = \frac{\rho_l RT}{M_v} \ln \left(\frac{-B + \sqrt{\Delta}}{2A} \right) \quad (16)$$

The Δ is given as $\Delta = B^2 - 4A(C - S_l \psi(\alpha) w_{max})$.

3.5 Evolution of the relative permeability

As mentioned in Section 2.2, $p_c(S_l, \alpha)$ is used to calculate k_{rl} and the results for CO are shown in Fig. 3. It can be seen that k_{rl} varies extremely little as a function of α . Thus, it would be possible to neglect the influence of α on k_{rl} . For each cement paste (CO, CN or CP) the simulation result k_{rl} at the age of 200 days is used for all ages.

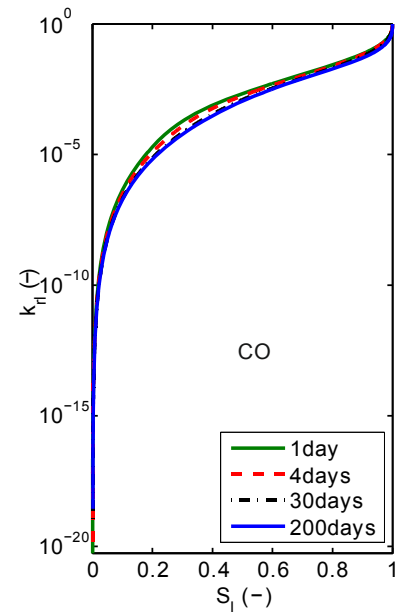


Fig. 3: The relative permeability at different ages.

4. RESULTS AND DISCUSSION

4.1 Drying kinetics

During the drying experiment, the cylindrical specimens, 7 cm diameter and 10 cm height, are sealed by adhesive aluminium foil sheets and only one side is exposed to the surrounding environment for 200 days drying. The characteristic parameters of specimens after one-day curing are gathered in Table 1, which are used for simulations. The method, the specimen dried at 105 °C and then saturated under vacuum condition, is used to measure the accessible-to-water porosity (ϕ). The degree of hydration is gained by thermogravimetric analysis (TGA). The Katz-Thompson relationship based on the percolation theory is employed to determine the intrinsic permeability [17, 18].

Fig. 4 presents the comparison of simulation results of mass loss kinetics and experiment results. It is shown that the model can manage to correctly simulate the drying kinetics of the specimens from early-age (1 day) up to 200 days.

4.2 Degree of hydration profiles

For OPC materials, the proportion of the calcium hydroxide ($\text{Ca}(\text{OH})_2$) to amounts of cement hydrate depends little on temperature and water-to-cement ratio [20] and a linear relationship between $\text{Ca}(\text{OH})_2$ content and degree of hydration could be found within the whole range of degrees of hydration according to experimental results [21]. In this research, $\text{Ca}(\text{OH})_2$ is considered to quantify the degree of hydration α at the early-age. The mass of $\text{Ca}(\text{OH})_2$ (m_{CH}) is determined by TGA measurement.

In order to show the influence of drying on hydration, degree of hydration profiles for CO and CP are presented in Figs. 5 and 6. The numerical results are obtained after different drying durations (1, 3, 7, 14, 28, 56, 120, and 200 days) and compared with measurements performed by TGA for each material (donated as symbols in each figure).

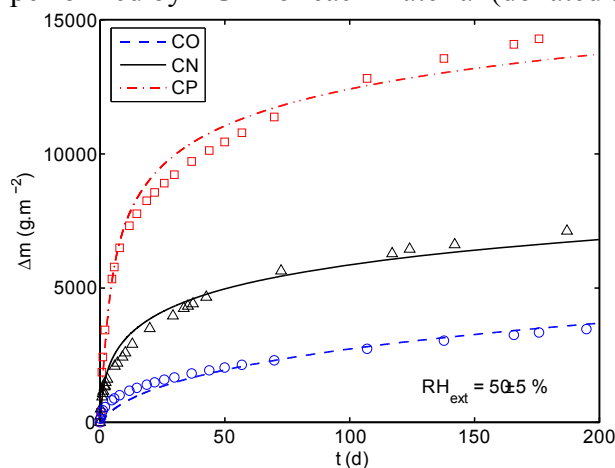


Fig. 4: Mass loss kinetics until 200 days. Simulations (lines) and experiments [4] (symbols).

Table 1: Summary of characteristic parameters of specimens.

Input data	CO	CN	CP
ϕ (%)	42.70	52.00	60.60
α_0 (-)	0.36	0.37	0.38
K_l^0 (10^{-20} m^2)	131	1093	5758
S_l^0 (-)	0.91	0.92	0.96

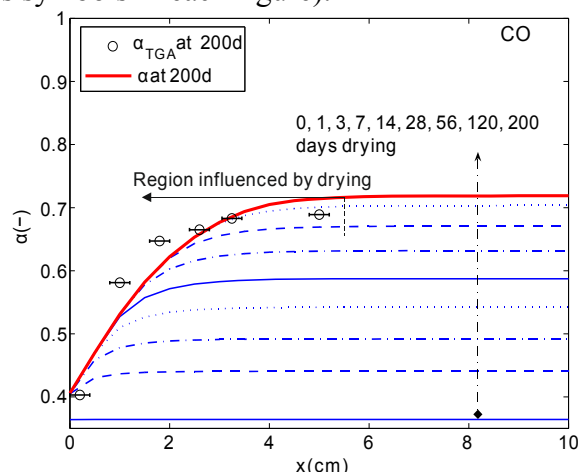


Fig. 5: Degree of hydration profiles for CO. TGA measurement [4] (symbols) and simulation results at 200 days (bold line).

The good agreement between the simulations and the experimental profiles indicates that the modelling leads to a relevant description of the coupling between hydration and moisture transfer. After 200 days of drying, the depth affected by the coupling is 4.5 cm for CO (see Fig. 5), while it almost corresponds to the total thickness for CP (10 cm, see Fig. 6). It proves the influence of external drying on the degree of hydration which increases with the rising of the water-to-cement ratio.

4.3 Porosity profiles

Fig. 7 shows the simulated porosity profiles (see Eq. (6)) for CO, CN and CP obtained after 200 days drying. These profiles are compared with gamma-ray attenuation measurement results.

The model provides a good prediction of the experimental porosity profiles from the surface to the core of the specimen. A comparison of degree of hydration profiles (Figs. 5 and 6) and microstructure (Fig. 7) shows that the influence of the early drying is more significant

in the vicinity of the exposed surface when the W/C ratio is low. For CO, the relative drop of the porosity near the surface reaches 46% whereas the relative decrease is only 24% for CP. This is because the different depth affected by drying for CO, CN and CP.

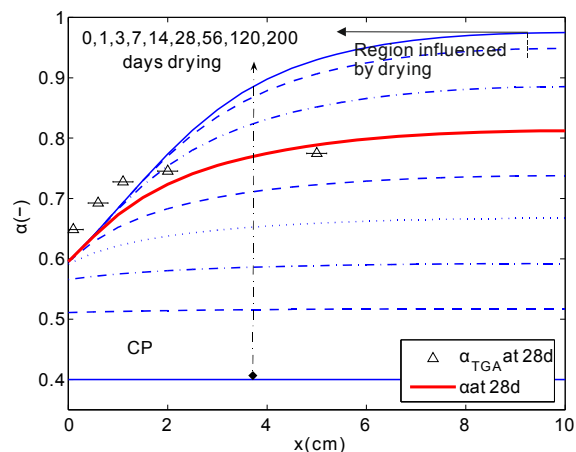


Fig. 6: Profiles of the degree of hydration for CP. TGA measurement [4] (symbols) and simulation results at 28 days (bold line).

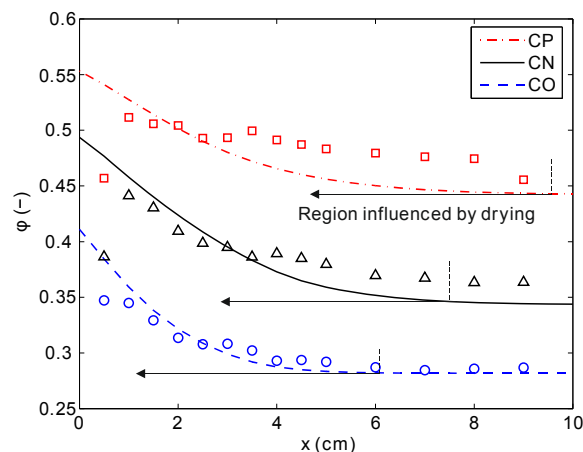


Fig. 7: Profiles of the porosity after 200-day drying. Simulations (lines) and experiments [4] (symbols).

In addition, since the evolution of porosity is linearly related to changes in the degree of hydration (see Eq. (6)), it is normal to observe that the porosity gradient reaches a depth equivalent to that reached by the degree of hydration (see Section 4.2).

5. CONCLUSIONS

A coupling model of hydration and drying is introduced in this paper. In this model, the degree of liquid water saturation and the degree of hydration are chosen as the main variables to describe the interactions between drying, hydration and the microstructure changes. The evolutions of the water vapor desorption curves, the porosity and the intrinsic permeability are expressed as a function of α . The proposed model is validated by the experimental data performed on three OPC pastes which are subjected to drying after one-day curing. A very good agreement is observed between the simulation results and the experimental data, as shown by the mass loss, degree of hydration and porosity profiles.

ACKNOWLEDGEMENTS

The research leading to these results has received funding from the European Union Seventh Framework Programme (FP7 / 2007-2013) under grant agreement 264448.

REFERENCES

- [1] Maekawa, K., Chaube, R. and Kishi, T. 'Coupled mass transport, hydration and structure formation theory for durability design of concrete structure', In Integrated design and environmental issues in concrete technology, 1995.
- [2] Bentz, D., Hansen, K., Madsen, H., Valle, F. and Griesel, E. 'Drying/hydration in cement pastes during curing', Materials and Structures, 34 (2001) 557-565.
- [3] Buffo-Lacarrere, L., Sellier, A., Escadeillas, G. and Turatsinze, A. 'Multiphase finite element modelling of concrete hydration', Cement and Concrete Research, 37 (2006)131-138.

- [4] Nguyen, M.D. 'Modelling the coupling between hydration and drying of cementitious materials after the formwork removal: Study of the degradation transfer properties (in French)', PhD thesis, ENPC, 2009.
- [5] Baroghel-Bouny, V. 'Water vapour sorption experiments on hardened cementitious materials. Part II. Essential tool for assessment of transport properties and for durability prediction', *Cement and Concrete Research*, 37(2007)438-454.
- [6] Daian, J.F. 'Condensation and isothermal water transfer in cement mortar part I: pore size distribution, equilibrium water condensation and imbibition', *Transport in Porous Media*, 3 (1988) 563-589.
- [7] Baroghel-Bouny, V. 'Water vapour sorption experiments on hardened cementitious materials. Part I. Essential tool for analysis of hygral behaviour and its relation to pore structure', *Cement and Concrete Research*, 37(2007)414-437.
- [8] Millington, R. 'Gas diffusion in porous media', *Science*, 130(1959)100-102.
- [9] Thiéry, M., Baroghel-Bouny, V., Bourneton, N., Villain, G. and Stefani, C. 'Modelling of drying of concrete: analysis of different modes of water transfer (in French)', *European Journal of Civil Engineering*, (2007)1-39.
- [10] Papadakis, V., Vayenas, C. and Fardis, M. 'Physical and chemical characteristics affecting the durability of concrete', *ACI Materials Journal*, 8(2) (1991)186-196.
- [11] Sercombe J., Vidal, R., Adenot, F., 'Gas diffusion in cement (in French)', *Transfer 2006*, Lille, Ecole Centrale, Fev. 2006.
- [12] Mualem, Y. 'A new model for predicting the hydraulic conductivity of unsaturated porous media', *Water Resources Research*, 12(1976)513-522.
- [13] Baroghel-Bouny, V., Thiéry, M. and Wang, X. 'Modelling of isothermal coupled moisture-ion transport in cementitious materials', *Cement and Concrete Research*, 41 (2011)828-841.
- [14] Bernard, O., Ulm, F.J. and Lemarchand, E. 'A multiscale micromechanics-hydration model for the early age elastic properties of cement-based materials', *Cement and Concrete Research*, 33(2003)1293-1309.
- [15] Fujii, K. and Kondo, W. 'Kinetics of the hydration of tricalcium silicate'. *Journal of The American Ceramic Society*, 57(1974)492-502.
- [16] Delmi, M., Aït-Mokhtar, A. and Amiri, O. 'Modelling the coupled evolution of hydration and porosity of cement-based materials', *Construction and Building Materials*, 20(2004)504-514.
- [17] Thompson, A., Katz, A. and Krohn, C. 'The microgeometry and transport properties of sedimentary rock'. *Advances in Physics*, 36(1987)625-694.
- [18] Thiéry, M., Villain, G. and Jaafar, W. 'Estimation of the permeability of cementitious materials by mercury porosimetry (in French)'. GFHN, Dijon, 24-26 November, 2003.
- [19] van Genuchten, M.Th. 'A close-form equation for predicting the hydraulic conductivity of unsaturated soils'. *Soil Science Society of America Journal*, (1980) 892-898.
- [20] Mounanga, P., Khelidj, A., Loukili, A. and Baroghel-Bouny, V. 'Predicting Ca(OH)_2 content and chemical shrinkage of hydrating cement pastes using analytical approach', *Cement and Concrete Research*, 34 (2004)255-265.
- [21] Baroghel-Bouny, V., Mounanga, P., Khelidj, A., Loukili, A. and Nouredine, R. 'Autogenous deformations of cement pastes Part II. W/C effects, micro-macro correlations, and threshold values', *Cement and Concrete Research*, 36 (2006)123-136.